Int J Adv Manuf Technol (2017) 90:2461–2476
DOI 10.1007/s00170-016-9567-3

ORIGINAL ARTICLE

Investigation of subsurface damage considering the abrasive particle rotation in brittle material grinding

Junkui Quan[1] · **Qihong Fang**[1] · **Jianbin Chen**[2] · **Chao Xie**[2] · **Youwen Liu**[1] · **Pihua Wen**[3]

Received: 26 April 2016 / Accepted: 6 October 2016 / Published online: 17 October 2016

Abstract Brittle materials are prone to brittle fracture which is a primary mechanism of material removal in grinding process. Subsurface damage (SSD) strongly affects the quality of grinding surface which is necessary to be evaluated in brittle material grinding. In this paper, the theoretical analysis of SSD is presented in detail considering the effect of abrasive particle rotation along with the wheel. With the increasing rotation angle of abrasive particle, both the median and lateral cracks incline gradually. Moreover, SSD could disappear below the final grinding surface when the rotation angle of abrasive particle reaches a certain critical value. In addition, the grinding depth, the wheel diameter, and the ratio of wheel speed to workpiece speed influence the rotation angle of an abrasive particle; the effects of these parameters on SSD depth are also studied in detail by theoretical analysis and numerical simulation. The larger wheel diameter and the larger ratio of wheel speed to workpiece speed can obtain a smaller SSD depth, but the effect of grinding depth is unapparent due to the kinematic characteristics of the grinding process. The results are meaningful and helpful in predicting SSD depth and selecting the reasonable grinding parameters to obtain a good surface quality in brittle material grinding.

✉ Qihong Fang
fangqh1327@hnu.edu.cn

[1] State Key Laboratory of Advanced Design and Manufacturing for Vehicle Body, Hunan University, Changsha 410082, People's Republic of China

[2] The Faculty of Mechanical Engineering and Mechanics, Ningbo University, Ningbo 315000, People's Republic of China

[3] School of Engineering and Material Sciences, Queen Mary, University of London, London E1 4NS, UK

Keywords Subsurface damage · Normal grinding force · Material removal rate · Abrasive particle rotation · Brittle materials

1 Introduction

Brittle materials have an increasingly wide utilization in the fields of semiconductor industry, medical, and micro-electromechanical based on their superior mechanical and structural properties such as high strength, high-temperature resistance, anticorrosive wearability, and light quality [1]. However, brittle materials tend to crack easily under small stress during machining due to their low fracture toughness. The major technological challenge is to achieve material removal through plastic deformation instead of the characteristic brittle fracture in machining of brittle materials [2]. The brittle fracture leads to subsurface damage (SSD) below the machining surface, which would strongly affect the mechanical properties and the service life of products [3].

In order to obtain a good workpiece surface quality, extensive studies have been undertaken to investigate the critical conditions for achieving ductile-mode grinding of brittle materials. Giovanola and Finnie [4] firstly proposed the viable scheme that material removal can be achieved by the ductile mode in the machining process of certain glasses similar to that in metals if cut depth is sufficiently small. Bifano et al. [5] presented that critical grinding depth for ductile-regime grinding of brittle materials is a function of intrinsic properties of the workpiece material. In machining brittle material in ductile mode, the undeformed chip thickness must be smaller than the cutting edge radius under a certain limit, which was studied by Cai et al. [6] and Liu et al. [7]. Cao et al. [8] investigated the material removal mechanism of SiC ceramics in ultrasonic-assisted grinding in detail using smooth particle

hydrodynamic (SPH) method and experimental test. Ductile chip formation is a result of large compressive stress in the cutting zone which suppresses the crack propagation and facilitates plastic deformation. Arif et al. [9] presented a model to predict critical undeformed chip thickness for ductile-brittle transition based on specific cutting energy, which indicated that the energy needed to propagate pre-existing flaws in the micro-structure of brittle materials is more than that needed to mobilize the micro-structural dislocations at such small scale of material removal, and hence plastic deformation is the primary mode during material removal process. Li et al. [10] investigated the mechanism of high-speed grinding to obtain the criterion of brittle-ductile removal transition of ceramics and achieve better surface quality and machining efficiency.

However, it is inevitable to propagate a crack under the machining surface when the machining condition is more than the critical condition of fracture free in machining brittle materials. As mentioned above, the workpiece surface of brittle material is often subjected to SSD when removing material in brittle fracture mode. Therefore, it is meaningful to investigate SSD depth as well as the influences of machining parameters on it during machining process in brittle fracture mode. Many studies were conducted based on indentation fracture mechanics to understand the grinding characteristics of BK7 [11, 12]. Lawn and Swain [13] depicted a general crack system of brittle materials in indentation process and reported that the crack system contained three crack styles: median, lateral, and radial cracks. Wang et al. [14] analyzed the influences of wheel speed, grinding depth, and apex angle of abrasive particle on SSD based on the kinematical characteristics in high-speed grinding process of brittle materials. Based on the grinding kinematics analysis and indentation fracture mechanism of brittle materials, Chen et al. [15] developed a new model to analyze the relationship between SR and SSD depth by considering the wheel spindle vibration, and their results indicated that the relationship is more or less affected by both grinding and vibration parameters.

Moreover, the normal force plays a significant role in material removal mode which affects SSD depth in the machining process of brittle materials. Lawn et al. [16, 17] developed a theory to establish the relationship between the load force with the evolution of median/lateral crack system based on a model in which the complex elastic-plastic field beneath the indenter is broken into elastic and residual components. The cutting force serves as a characteristic to describe the stone machining process because it significantly influences tool wear, the cutting temperature, the residual stress, and the surface integrity [18]. Agarwal and Rao [19, 20] reported that the grinding force is a significant quantitative indicator to describe the material removal mode because it strongly affects specific grinding energy and surface damage. The grinding force and the surface generation in micro-grinding of ceramic material were studied using the finite element method (FEM) and the experiment test by Feng et al. [21]. Gu et al. [22, 23] discovered that there is a linear relationship between the normal load and the square of scratch depth and studied the effect of the normal load on the characteristics of chipping behaviors and material removal mechanism in the brittle fracture mode during scratch process of BK7 glasses. Wang et al. [24] investigated the material removal rate of single abrasive particle and the grinding force in brittle material grinding utilizing theoretical analysis and numerical simulation. Huang et al. [25] and Chen et al. [26] studied the relationship between the grinding force and grinding parameters through experimental method. In recent years, the cutting force was directly studied under the assumption that brittle fracture is the dominant mechanism of material removal in rotary ultrasonic face milling of brittle materials, and the effects of machining parameters on that also were analyzed both theoretically and experimentally [27–29].

In those studied above, there are a few papers and no detailed investigations on SSD depth in brittle fracture mode considering the effect of abrasive particle rotation along with the wheel during brittle material grinding. Unlike the single abrasive particle scratch process, the rotation angle of abrasive particle during the grinding process will influence SSD depth which determines the critical conditions for brittle-ductile transition. Therefore, the objective of this study is to theoretically analyze SSD depth by considering the effects of both abrasive particle rotation along with the wheel and some significant grinding parameters and which will be validated by numerical simulation.

2 Theoretical analysis of SSD depth in brittle material grinding

In general, there are two material removal modes in grinding process of hard and brittle materials, the brittle fracture and ductile modes. Liu et al. [27] believed that the brittle fracture is the primary mechanism of material removal in machining of brittle materials. The abrasive particle cutting the workpiece surface causes the initiation and propagation of the lateral and median cracks in brittle material grinding, which leads to material removal in brittle fracture mode and chip formation [28]. The typical crack systems in brittle material scratching by abrasive particle are shown in Fig. 1. The lateral crack length C_l and median crack length C_m are the two main forms to evaluate SSD in brittle material grinding [30]. SSD strongly influences the mechanical strength and subsurface quality of the brittle components during the grinding process [14]. Therefore, the relationship between SSD depth and grinding parameters should be analyzed to obtain the crack-free workpiece surface.

2.1 Analysis of the length and depth of lateral cracks

Lateral cracks were observed to initiate near the base of the plastic deformation zone below the contact surface and to

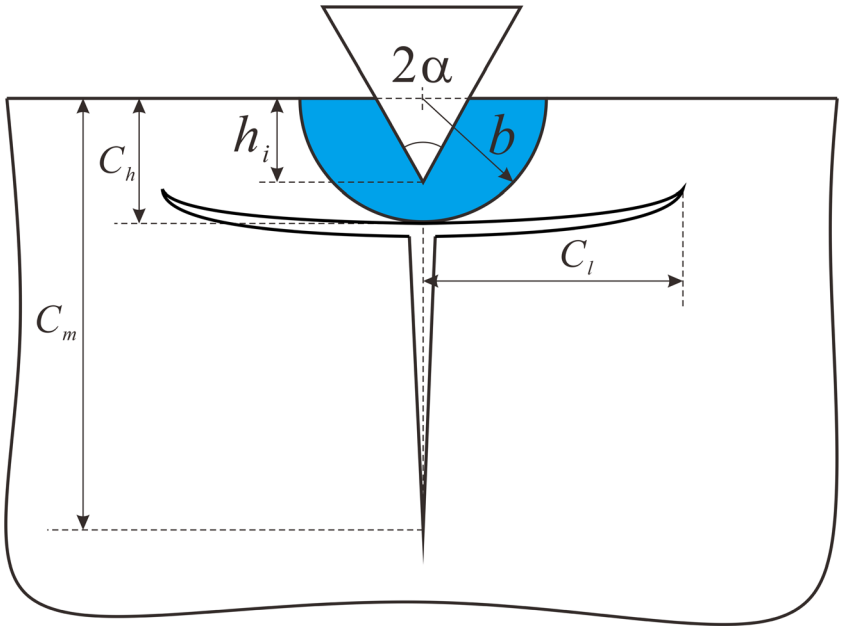

Fig. 1 Typical crack systems in brittle materials scratching by abrasive particle

spread out laterally on a plane closely parallel to the specimen surface by Lawn and Wilshaw [31]. The length of lateral cracks C_l and the depth of lateral cracks C_h had been depicted by Marshall et al. [17].

$$C_l = k\cdot(\cot\alpha)^{\frac{5}{12}}\cdot\left(\frac{E^{\frac{3}{4}}}{H_s K_c(1-\nu^2)^{\frac{1}{2}}}\right)^{\frac{1}{2}}\cdot F_n^{\frac{5}{8}} \tag{1}$$

$$C_h = k\cdot(\cot\alpha)^{\frac{1}{3}}\cdot\frac{E^{\frac{1}{2}}}{H_s}\cdot F_n^{\frac{1}{2}} \tag{2}$$

where C_l is the lateral crack length; C_h is the lateral crack depth; K_c the fracture toughness of the workpiece materials; H_s the hardness of the workpiece materials; E the elastic modulus of the workpiece materials; ν the Poisson's ratio of the workpiece materials; F_n the normal load of single abrasive particle during the grinding process; α the half apex angle of abrasive particle; and k the dimensionless constant which is dependent on the material/indenter system, $k = 0.226$ [17].

In the grinding process of brittle materials, the lateral crack depth and length significantly influence the actual material removal volume of single abrasive at the workpiece grinding surface, which leads to the complexity in depicting and calculating the volume of single abrasive particle in removing material. Therefore, for the convenience of evaluating material removal volume by single abrasive particle, it is necessary to establish some reasonable assumptions and simplifications in the grinding process of brittle materials, and the major assumptions and simplifications are carried out as follows:

1. Ignore the vibration of wheel and workpiece in the grinding process of brittle materials, and grinding process of single abrasive particle is carried out continuously.
2. All abrasive particles involved in brittle material grinding are assumed to be rigid with the shape of a circular cone in grinding process.
3. The material removal volume of single abrasive particle in the whole grinding process in brittle fracture mode can be regarded as a rectangular pyramid as shown in Fig. 2, and the bottom surface area of the rectangular pyramid is determined by the length and the depth of lateral cracks.

According to the assumptions and the simplifications above as well as the shape of an undeformed chip by single abrasive particle in brittle fracture mode in Fig. 2, the material removal volume by single abrasive particle in grinding process can be given as follows:

$$V = \frac{1}{3}\cdot 2C_l\cdot C_h\cdot L_s \tag{3}$$

where L_s is the contact trajectory length between the wheel and workpiece and given by Marinescu et al. [32]

$$L_s = \left(a_p d_e\right)^{\frac{1}{2}} \tag{4}$$

with a_p being the grinding depth and d_e the equivalent diameter of the wheel and given by

$$d_e = d_w\left(1 \pm \frac{v_w}{v_s}\right)^2 \tag{5}$$

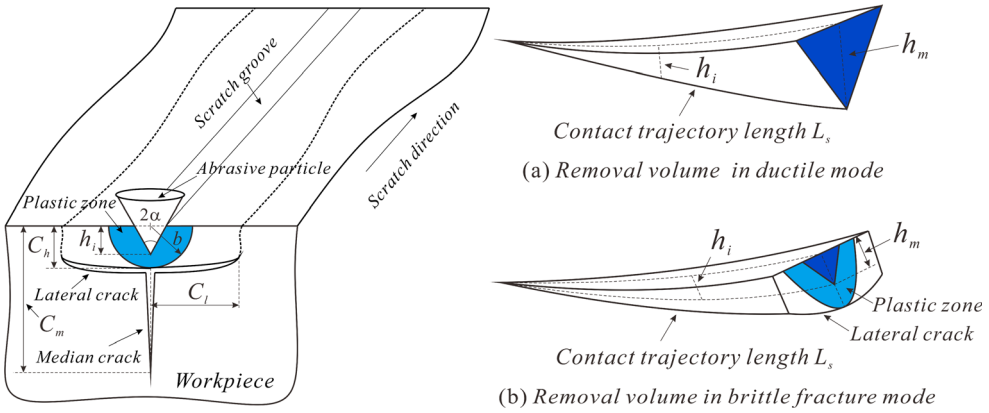

Fig. 2 Schematic of scratching brittle materials by abrasive particle (*left*) and three-dimensional shape of removal volume in two grinding mode: **a** ductile mode and **b** brittle fracture mode

where plus and minus signs are used for up-grinding and down-grinding, respectively; d_w is the diameter of the wheel; v_s is the constant peripheral speed of the wheel against a moving workpiece; and v_w is the relative constant workpice speed.

In the grinding process of brittle materials, the product of removal material volume V of single abrasive particle with all the numbers N of the abrasive particle in per unit width of the wheel's contact arc equals to the total material removal volume (MRV) of the wheel's per unit width in brittle fracture mode during the effective grinding time Δt. Hence, MRV can be obtained by the following equation considering the continuity analysis by Malkin [33].

$$\mathrm{MRV} = N \cdot V \tag{6}$$

All numbers of active abrasive particle N in contact arc per unit width can be expressed by the equation:

$$N = C \cdot v_s \cdot \Delta t \tag{7}$$

where C is the number of active abrasive particle per unit area and C = 3.2 grit/mm^2 for the 50/60 grit wheel is estimated from micrographs of the wheel surface by using an optical microscope [26].

In addition, MRV in the actual grinding process can be expressed by the product of grinding depth and workpiece speed in the effective time Δt.

$$\mathrm{MRV} = a_p \cdot v_w \cdot \Delta t \tag{8}$$

Therefore, by substituting Eqs. (6) and (7) into Eq. (8), we can get the equation:

$$N \cdot V = a_p \cdot v_w \cdot \Delta t \tag{9}$$

That is as follows:

$$C \cdot v_s \cdot \frac{2}{3} k (\cot\alpha)^{\frac{5}{12}} \left(\frac{E^{\frac{3}{4}}}{H_s K_c (1-\nu^2)^{\frac{1}{2}}} \right)^{\frac{1}{2}} F_n^{\frac{5}{8}} \cdot k (\cot\alpha)^{\frac{1}{3}} \frac{E^{\frac{1}{2}}}{H_s} F_n^{\frac{1}{2}} \cdot (a_p d_e)^{\frac{1}{2}} = a_p v_w \tag{10}$$

From Eq. (10), the normal grinding force of single abrasive particle in brittle fracture mode can be expressed by the following equation:

$$F_n = \left[\frac{3(\tan\alpha)^{\frac{3}{4}}}{2Ck^2} \frac{H_s^{\frac{3}{2}} K_c^{\frac{1}{2}} (1-\nu^2)^{\frac{1}{4}}}{E^{\frac{7}{8}}} \frac{v_w}{v_s} \left(\frac{a_p}{d_e} \right)^{\frac{1}{2}} \right]^{\frac{8}{9}} \tag{11}$$

Therefore, the values of C_l and C_h can be obtained by substituting Eq. (11) to Eqs. (1) and (2), respectively.

2.2 Analysis of the depth of median cracks

In the grinding process of brittle materials, with increasing the abrasive particle depth h_i penetrating into the workpiece surface of brittle materials, a plastic deformation zone emerges beneath the abrasive particle tip and a high residual stress is under the plastic deformation zone to conserve the volume [2]. Generally speaking, previous studies indicated that brittle material removal is by the formation of a lateral crack in the brittle fracture mode, and lateral cracks were observed to initiate near the base of the plastic deformation zone below the contact surface and followed by the subsequent propagation on the plane closely parallel to the workpiece surface [31, 34], which would lead to a complete material removal under the contact surface in brittle material grinding. In addition, when the penetration depth of abrasive particle h_i is larger than the critical undeformed chip thickness h_c, which is $h_i > h_c$, the median crack would emerge perpendicularly to the grinding surface, and it is considered the main type of surface cracks according to Nakamura et al. [35].

The critical undeformed chip thickness h_c was proposed by Bifano et al. [5]

$$h_c = 0.15 \frac{E}{H_s} \left(\frac{K_c}{H_s} \right)^2 \tag{12}$$

Based on the indentation of sharp indenter according to the micro-indentation mechanics as well as the relationship

between indentation and scratch process, the relationship between median crack length and scratch depth was established by Gu et al. [36]:

$$C_{\mathrm{m}} = 0.206\frac{(EH_{\mathrm{s}})^{\frac{1}{3}}}{(K_{\mathrm{c}}\beta)^{\frac{2}{3}}}(\cot\alpha)^{\frac{4}{9}}(\tan\alpha)^{\frac{4}{3}}\cdot h_{\mathrm{i}}^{\frac{4}{3}} \tag{13}$$

where β is a material parameter determined by elastic recovery, and $\beta = 0.329$ [37].

The penetration depth h_{i} can be expressed based on the kinetic relationship between the wheel and the workpiece by Marinescu et al. [32]:

$$h_{\mathrm{i}} = \frac{h_{\mathrm{m}}}{2}\left(\frac{d_{\mathrm{e}}}{a_{\mathrm{p}}}\right)^{\frac{1}{2}}\theta_{\mathrm{i}} \tag{14}$$

where θ_{i} is the rotation angle of abrasive particle along with the wheel shown in Fig. 3, and the range of the rotation angle θ_{i} from 0 to the maximum value θ_{m}; h_{m} is the maximum penetration depth of abrasive particle or the maximum undeformed chip thickness.

The maximum rotation angle θ_{m} can be expressed by Marinescu et al. [32]:

$$\theta_{\mathrm{m}} = \arcsin\left[2\left(\frac{a_{\mathrm{p}}}{d_{\mathrm{e}}}\right)^{\frac{1}{2}}\right] \tag{15}$$

In addition, the maximum penetration depth h_{m} depends on the relationship between the wheel and the grinding parameter, which can be expressed by Shaw [38]:

$$h_{\mathrm{m}} = \left[\frac{4}{Cr}\frac{v_{\mathrm{w}}}{v_{\mathrm{s}}}\left(\frac{a_{\mathrm{p}}}{d_{\mathrm{e}}}\right)^{\frac{1}{2}}\right]^{\frac{1}{2}} \tag{16}$$

where r is the ratio of the cross-sectional width and thickness of the chip, and the value is given by $r = 10$ [39].

2.3 The effect of abrasive particle rotation on SSD depth

In the grinding process of brittle materials, the cracks are distributed in the contact zone between the abrasive particle and the workpiece materials. When the abrasive particle rotates along with the wheel, the cracks gradually incline which could change the crack depth penetrating into the final grinding surface, even the cracks could disappear below the final grinding surface when the crack inclination angle reaches a certain value. Therefore, the effect of abrasive particle rotation on SSD depth should be considered in detail in brittle material grinding, because this could enlarge the critical undeformed chip thickness in brittle-ductile transition to some extent. A simplified schematic diagram of this grinding process is shown in Fig. 3.

In addition, some factors affecting the rotation angle are also required to be considered. The grinding wheel diameter plays an important role in the grinding process in order to obtain high machining accuracy and good surface quality of the workpiece [40–42]. In the grinding process, the maximum rotation angle of abrasive particle is closely related with the wheel diameter. Under a certain grinding depth, the smaller the wheel diameter leads to the larger the rotation angle of abrasive particle, which can be clearly shown in Fig. 4. Moreover, the grinding depth a_{p} and the $v_{\mathrm{s}}/v_{\mathrm{w}}$ ratio can also influence the rotation angle of abrasive particle in the grinding process.

When the penetration depth of abrasive particle gradually increases and reaches the critical depth of the occurrence of brittle-ductile transition, which is $h_{\mathrm{i}} > h_{\mathrm{c}}$, the cracks could

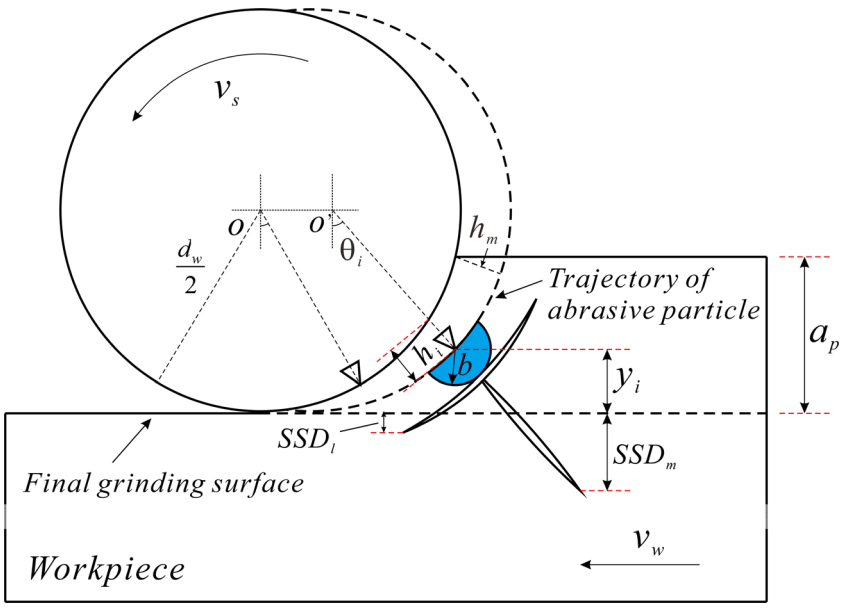

Fig. 3 Brittle crack inclines with abrasive particle rotation in grinding process of brittle materials

penetrate into the final grinding surface. Since the direction of median cracks and lateral cracks is determined by the rotation angle, and according to Eqs. (12) and (14), the critical brittle fracture angle θ_c could be obtained.

$$\theta_c = \frac{2h_c}{h_m}\left(\frac{a_p}{d_e}\right)^{\frac{1}{2}} \tag{17}$$

When the rotation angle θ_i is more than the critical brittle fracture angle θ_c during the grinding process of brittle materials, the crack could emerge in the contact surface.

2.4 Evaluating SSD depth induced by median or lateral cracks

As shown in Fig. 3, y_i represents the distance of the tip of abrasive particle to the final grinding surface, which can be calculated as follows:

$$y_i = \frac{d_e}{2}(1-\cos\theta_i) \tag{18}$$

Median and lateral cracks could lead to SSD in brittle material grinding, and SSD depth is determined by the median crack length and the lateral crack length as well as the rotation angle of the abrasive particle from Fig. 3. In the model of this paper, SSD_m represents SSD depth caused by median cracks and SSD_l represents SSD depth caused by lateral cracks. The final SSD depth is determined by the bigger one of them in brittle material grinding. Based on the geometrical relationship in Fig. 3, SSD_m and SSD_l can be expressed as follows:

$$SSD_m = (C_m - h_i)\cos\theta_i - y_i \tag{19}$$

$$SSD_l = (C_h - h_i)\cos\theta_i + C_l\sin\theta_i - y_i \tag{20}$$

3 Results and discussion

In this paper, the optical glass of BK7 is considered to analyze SSD and evaluate its depth. The material properties of BK7 are shown in Table 1 according to the works of Gu et al. [23].

3.1 The effects of grinding parameters on the normal grinding force

When the material removal process is in brittle fracture mode, the normal grinding force of a single abrasive particle is required to significantly consider obtaining the length and depth of lateral cracks. The normal grinding force is closely relative to the grinding parameters from Eq. (11), such as grinding depth, wheel diameter, the v_s/v_w ratio, and the half apex angle of abrasive particle α. The normal grinding force increases with the increasing grinding depth as shown in Fig. 5a, which is because when grinding depth is increased, the material removal rate also increases, and hence the larger normal

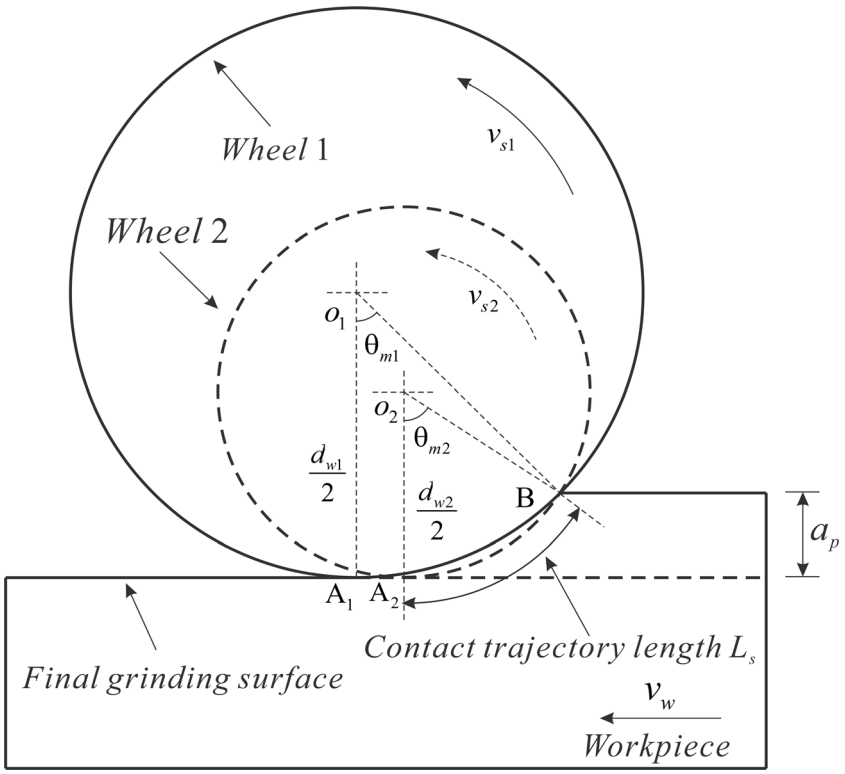

Fig. 4 The maximum rotation angle of abrasive particle θ_m versus different wheel diameters d_w

Table 1 Material properties of BK7

Parameters	Values
Young's modulus E (GPa)	82
Poisson's ratio ν	0.203
Vickers hardness H_s (GPa)	7.7
Fracture toughness K_c (MPam$^{1/2}$)	0.82

grinding force is required in the material removal process. Figure 5b depicts that the normal grinding force decreases as the wheel diameter increases. The reason could be that the larger grinding wheel diameter leads to the reduction in material removal rate of a single abrasive particle according to the works of Jackson et al. [43], which can be explained well in the works of Hecker and Liang [44], indicating that a chip thickness of each abrasive particle reduction exists in the grinding process due to the higher number of abrasive particles in the contact area between the larger wheel and the workpiece. Hence, the corresponding material removal volume of single abrasive particle reduces, which leads to the reduction in the normal grinding force of the single abrasive particle with the increasing wheel diameter for a given material properties according to Eqs. (1) to (3) in the present paper. Figure 5c presents that the normal grinding force decreases with the increasing v_s/v_w ratio. That is to say that the grinding force decreases with the increasing wheel speed for a given workpiece speed and increases with the increasing workpiece speed for a given wheel speed. The reason is that elevating the v_s/v_w ratio is equivalent to a decrease in the penetration depth of each abrasive particle engaged in material removal process, leading to the reduction in material removal volume of a single abrasive particle. In addition, the apex angle of abrasive particle is investigated in the present study to better understand the effect of abrasive particle size on the grinding process of brittle materials. Figure 5d indicates that the normal grinding force increases with the increment of the half apex angles of abrasive particle α, which means that the normal grinding force increases with the increase of the abrasive particle size. The reason may be that the penetration depth of abrasive particle increases with the increasing apex angle of abrasive particle according to the works of Li and Liao [45], which leads to an increase in material removal volume of abrasive particle.

As mentioned above, the normal grinding force increases with the increment of grinding depth and workpiece speed, whereas decreases with the increasing wheel speed, which are consistent with existing studies using theoretical and experimental methods by Huang et al. [25], Liu et al. [27], and Zhang et al. [28]. Park and Liang [46] proposed that the wheel diameter affects the physical mechanisms of material removal process, and their results indicated that the grinding force decreases with the increasing wheel diameter, which proves the correctness of the present analysis results regarding the effect of grinding wheel diameter on normal grinding force.

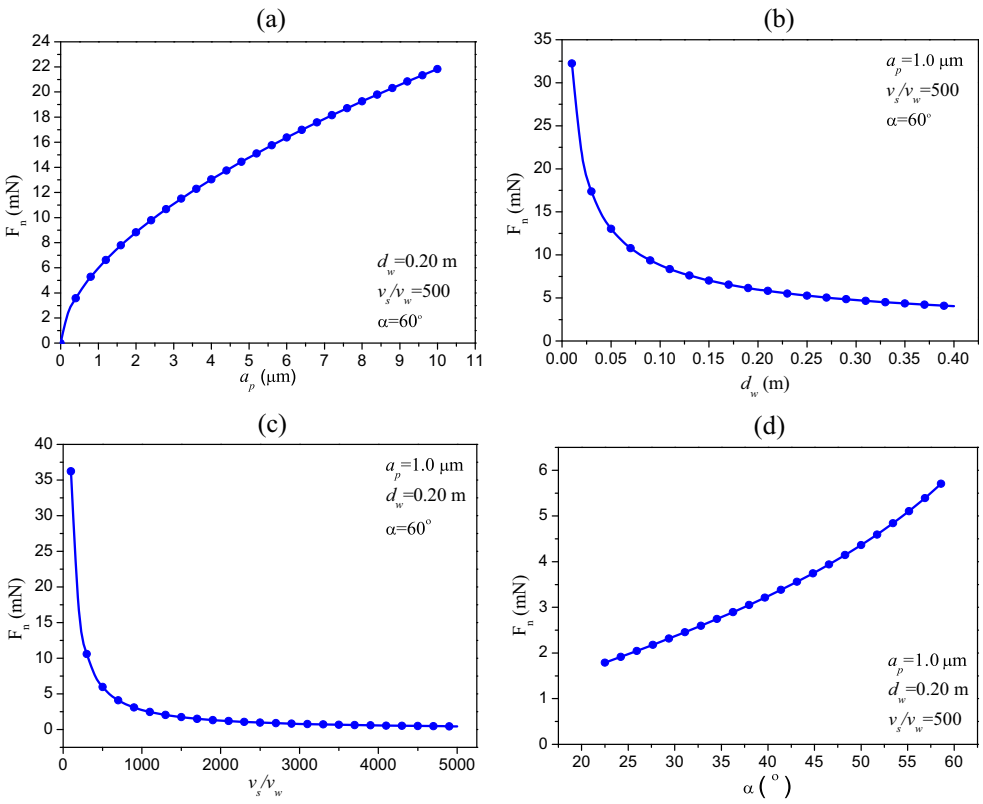

Fig. 5 The normal grinding force of abrasive particle versus different parameters: **a** the grinding depth a_p, **b** the wheel diameter d_w, **c** the ratio v_s/v_w, and **d** the half apex angle of abrasive particle α

Moreover, the results from the works of Hecker and Liang [44] presented the larger grinding wheel diameter which leads to a lower surface roughness, which can also indirectly validate the normal grinding force that reduces with the increment of grinding wheel diameter. The reason is that the depth of lateral cracks expressed by Eq. (2) in the theoretical analysis above is often regarded as the surface roughness in final grinding surfaces without considering the abrasive particle rotation, and is only determined by the normal grinding force for a given material properties in brittle material grinding.

3.2 The effects of grinding parameters on SSD depth

The optimal grinding mode is that grinding parameters are rationally selected to make material removal process in fracture-free mode. Therefore, the critical brittle fracture angle θ_c is a meaningful factor to evaluate the brittle-ductile transition in the grinding process, which can be influenced by the grinding depth, the v_s/v_w ratio, and the grinding wheel diameter according to a previous analysis. Figure 6a–c shows the trends of critical brittle fracture angle θ_c under different grinding parameters and the cracks that emerge below the grinding surface, which indicate that the critical brittle fracture angle θ_c increases with the increment of grinding depth and the v_s/v_w ratio, whereas decreases with the increasing wheel diameter. That is to say that the larger grinding depth and the v_s/v_w ratio as well as the smaller wheel diameter are beneficial to extend the length of ductile processing and delay the ductile processing in translating to brittle processing.

The median crack and the lateral crack are the main types of SSD in brittle material grinding. Wang et al. [14] have developed a predictive model to analyze SSD depth induced by median cracks. However, based on kinematic characteristics of the grinding process and taking the rotation angle of abrasive particle into account, lateral cracks also could penetrate into the grinding surface which leads to SSD, and almost no attention to this aspect in evaluating SSD existed in other papers. Therefore, in the present study, SSD depth is evaluated comprehensively by the depth of median cracks and lateral cracks penetrating into the grinding surface with the consideration of abrasive particle rotation along with the wheel.

3.2.1 The effect of the grinding depth a_p

Figure 7 shows SSD depth under different grinding depths a_p based on the kinematic characteristics of the grinding process in brittle fracture mode. Figure 7 indicates that SSD_m increases with the increment of rotation angle for a certain grinding depth (such as $a_p < 5$ μm), and reaches the maximum SSD_m when $\theta_i = \theta_m$. However, for a larger grinding depth (such as $a_p > 5$ μm), SSD_m firstly increases to the peak value, and then gradually decreases with the increment of rotation angle. Even when $a_p = 10$ μm, SSD_m finally is less than zero, indicating that SSD disappears below the final grinding surface, which illustrates that the effect

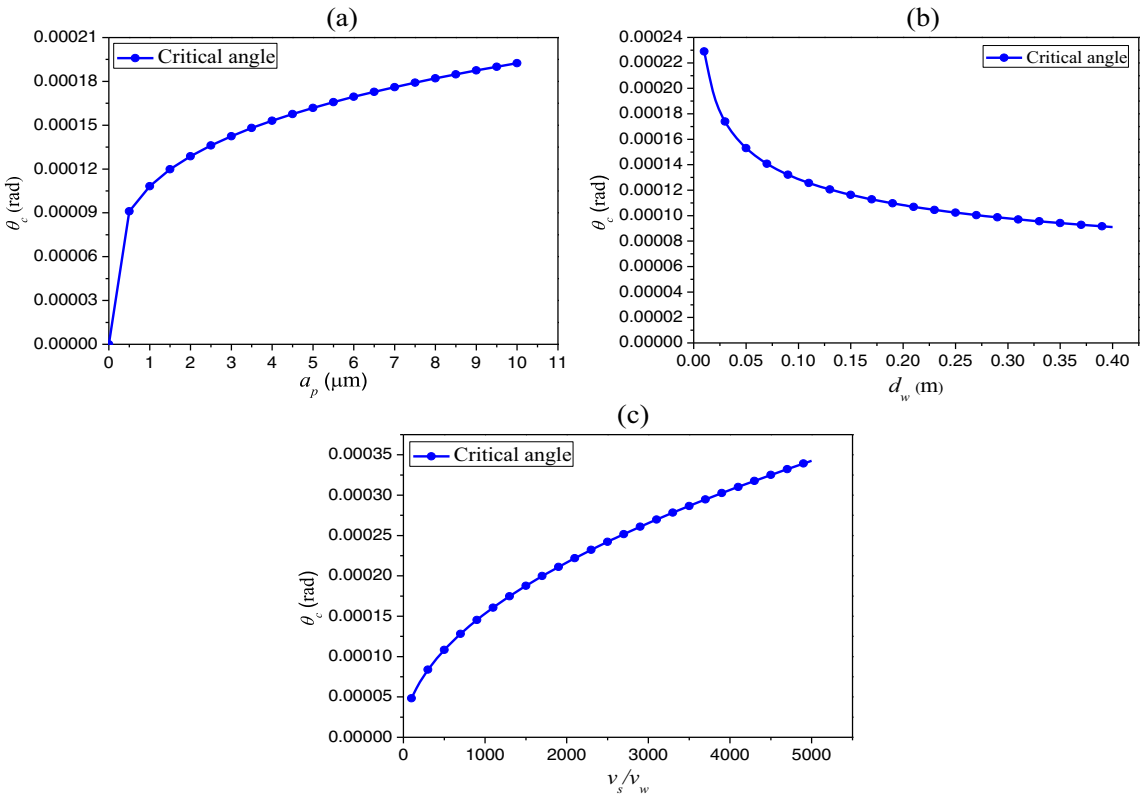

Fig. 6 The critical brittle fracture angle θ_c versus different parameters: **a** the grinding depth a_p, **b** the wheel diameter d_w, and **c** the ratio v_s/v_w

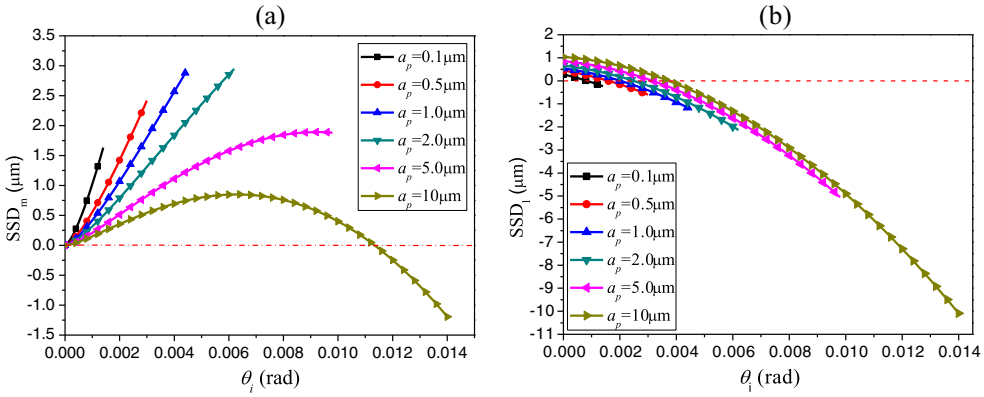

Fig. 7 Effects of different a_p on SSD_m (**a**) and SSD_l (**b**)

of grinding depth on SSD_m is unapparent. In addition, the propagation of lateral cracks is closely parallel to the grinding surface in brittle material grinding; hence, the lateral crack tip could also extend to the final grinding surface with the increment of rotation angle. With the increment of rotation angle, SSD_l decreases and finally reaches less than zero in Fig. 7b, which indicates that SSD induced by lateral crack disappears below the final grinding surface. Since the critical brittle fracture angle θ_c is very little during the grinding process as shown in Fig. 6, the ductile process can be ignored and the brittle fracture mode can be regarded as the primary mechanism in this grinding process. The initial value of SSD_l increases with the increasing grinding depth, which may be due to the fact that the increasing normal grinding force leads to a longer length of lateral cracks.

3.2.2 The effect of the grinding wheel diameter d_w

With the increasing wheel diameter in grinding process, the contact trajectory length L_s increases but the maximum rotation angle θ_m decreases as seen in Fig. 4, and the distance y_i of abrasive particle tip to the final grinding surface increases according to Eq. (18), which has a significant influence on SSD depth. The effect of the wheel diameter on SSD depth is plotted in Fig. 8, which shows a good agreement with the experimental results [44]. It can be discovered that the smaller wheel diameter leads to the larger SSD_m in Fig. 8a. Moreover, when the wheel diameter is in the range of 0.05 to 0.4 m, SSD_m does not present a decline trend with the increment of rotation angle. Figure 8b depicts the trends of SSD_l for different wheel diameters, which are similar to the effect of the grinding depth. With the increment of rotation angle, SSD_l gradually decreases and finally reaches less than zero. The larger wheel diameter leads to the smaller critical rotation angle that SSD_l is equal to zero, which indicates that the larger wheel diameter is beneficial to obtain a good quality of grinding surface in brittle material grinding.

3.2.3 The effect of the v_s/v_w ratio

In brittle regime of brittle material grinding, both wheel speed and workpiece speed are key factors that affect the quality of the workpiece surface. High wheel speed in conjunction with a high workpiece speed is a crucial means for the brittle to ductile transition, leading to a desired surface morphology and residual stress distribution [47]. For a given rotation angle, the higher wheel speed v_s causes the smaller undeformed chip thickness h_i which makes the median crack length smaller, and the higher workpiece speed v_w leads to the larger material removal volume V which makes the lateral crack length larger. The effect of the v_s/v_w ratio on SSD depth has been analyzed in detail as shown in Fig. 9, which is consistent with the experimental results by Hecker and Liang [44].

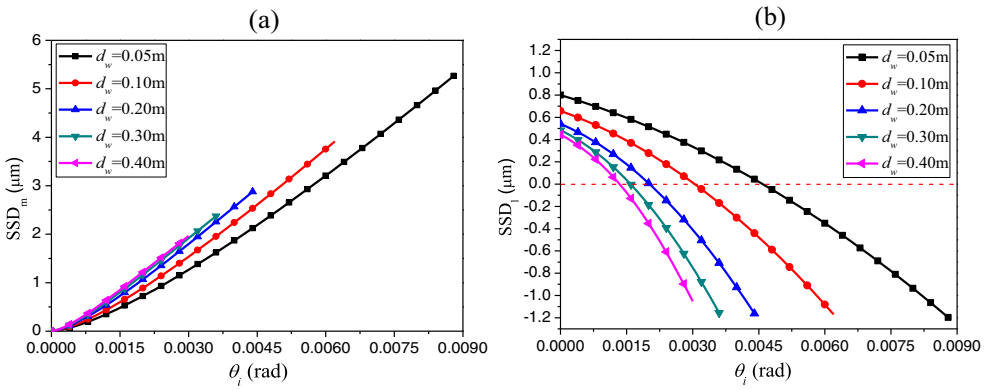

Fig. 8 Effects of different d_w on SSD_m (**a**) and SSD_l (**b**)

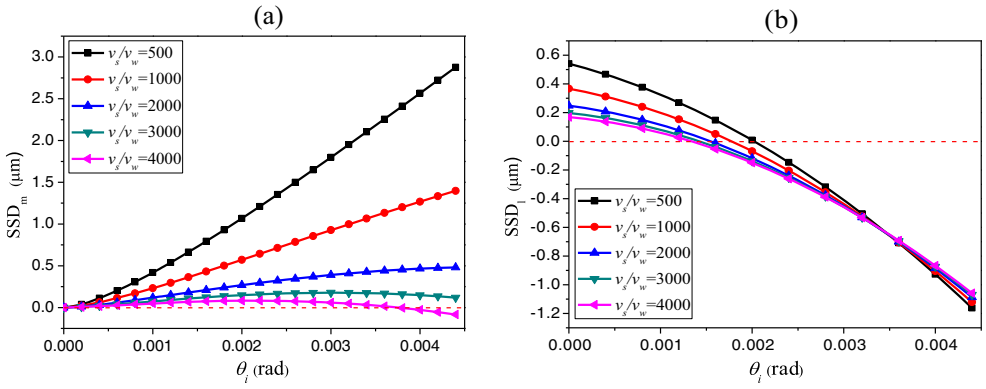

Fig. 9 Effects of different v_s/v_w on SSD_m (**a**) and SSD_l (**b**)

Figure 9 a presents that SSD_m decreases with the increment of the v_s/v_w ratio. For a large value of the v_s/v_w ratio (for example, v_s/v_w = 4000), with the increment of the rotation angle, SSD_m firstly increases and then decreases, finally is less than zero. Figure 9 b shows the effect of the v_s/v_w ratio on SSD_l. With the increment of the rotation angle, SSD_l is decreased gradually and finally is less than zero. For a larger v_s/v_w ratio, SSD_l and the critical rotation angle (SSD_l is equal to zero) are smaller than a lower v_s/v_w ratio. Moreover, it can be observed from Fig. 9 that SSD_m and SSD_l decrease with the increasing wheel speed for a given workpiece speed, and meanwhile increase with the increasing workpiece speed for a given wheel speed. According to the analysis above and the work of Inasaki [48], if wheel speed v_s and workpiece speed v_w increase, keeping in the same proportion which makes the v_s/v_w ratio be at a given constant has no effect on quality of the grinding surface, but the higher grinding efficiency can be obtained in the grinding process. Therefore, the proper larger v_s/v_w ratio is beneficial to obtain a high efficiency and a good surface integrity, which is helpful in actual brittle material grinding.

The theoretical analysis results of SSD are depicted considering the effect of abrasive particle rotation during the grinding process of BK7 glass from Figs. 7, 8, and 9. According to the above analysis, it can be clearly seen that SSD_l being the main factor that dominates SSD only worked in the initial state of the grinding process. However, as the penetration depth of abrasive particle increases, SSD_m gradually increases and finally replaces SSD_l as the main factor that dominates SSD. In addition, some of the experimental tests have been implemented to investigate subsurface damage in brittle material grinding without considering the abrasive particle rotation. The experimental results from Yao et al. [30], Gu et al. [37], and Chen et al. [49] indicated that SSD increases with the increment of workpiece speed, whereas decreases with the increment of wheel speed. Hecker and Liang [44] investigated the surface roughness which indicated that the surface roughness decreases with the increasing wheel diameter. But for the grinding depth in the present theoretical model with the consideration of abrasive particle rotation, the trend of SSD is no longer a pure increase or decrease due to the fact that median and lateral cracks incline with the rotation of abrasive particle. Therefore, the present theoretical model is more accurate in predicting and controlling the SSD in actual brittle material grinding. As mentioned above, the present theoretical results are in good agreement with those existing experimental works to a certain extent.

3.3 Numerical simulations of the grinding process of BK7

Grinding is a material removal process where multiple abrasive particles are engage in the workpiece [50]. This paper

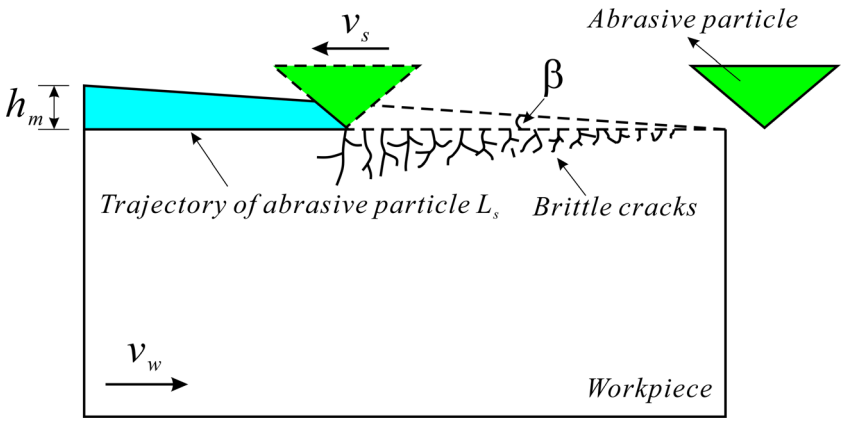

Fig. 10 Simulation schematic in grinding process of BK7

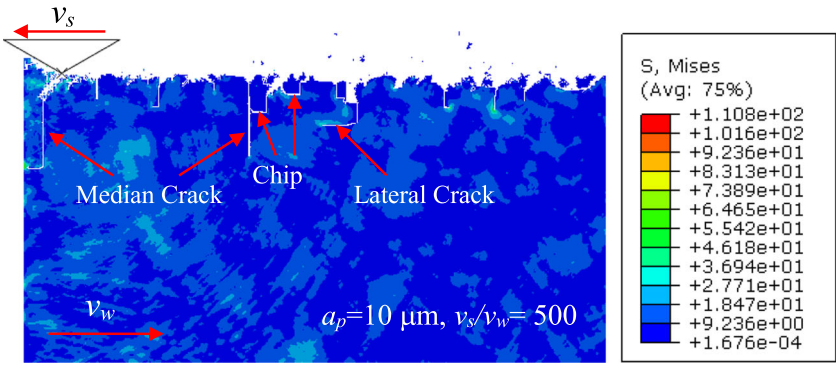

Fig. 11 Surface morphology in grinding simulation process of BK7 glass

utilized finite element method (FEM) to simulate two-dimensional model of the BK7 grinding process by single abrasive particle in *brittle cracking model* available in ABAQUS/Explicit [51]. In the simulation, the abrasive particle is assumed to be rigid, and the element type CPE4RT is utilized to divide the mesh of the workpiece. In order to analyze the effect of abrasive particle rotation in brittle material grinding, an inclined angle determined by the locations of start point and cut out point of abrasive particle is assumed to replace the process of abrasive particle rotation along with the wheel in the simulation process. As shown in Fig. 10, h_m is the maximum penetration depth that depends on the grinding depth a_p, a difference of which can be utilized to investigate the effect of grinding depth on SSD depth in simulation. In addition, according to Eq. (15), the effect of wheel diameter on SSD depth can be presented by changing the maximum rotation angle θ_m for a given a_p. Figure 11 shows surface morphology by grinding simulation process of BK7 glass, and median and lateral cracks can be clearly presented in the simulation process. It can be discovered that lateral cracks are the main factors that lead to the chip formation, and the chip shape can be approximately regarded as quadrilateral, which is consistent with previous assumptions. The grinding parameters in simulation are shown in Table 2.

The grinding depth plays a significant role in SSD depth in brittle material grinding from Fig. 7. Figure 12a–d shows the simulation process under different grinding depths which are respectively a_p = 1, 2, 5, and 10 μm, which determined that the corresponding maximum penetration depths are 0.75, 0.89, 1.12, and 1.33 μm. The maximum crack depths by simulation process are measured, which respectively are 5.47, 7.8, 8.5, and 9.7 μm. Therefore, the crack depth is increased with the increasing grinding depth, which is qualitatively similar to the simulation process of SiC grinding by Zhu et al. [47]. Moreover, according to Eq. (19), the corresponding SSD depths during the simulation process of BK7 glass obtained are 3.75, 4.98, 2.56, −1.47 μm. The curve is shown in Fig. 14a, which reveals that SSD depths are not always increased with the grinding depth, even if SSD depth is less than zero, cracks disappear below the grinding surface of workpiece at a_p = 10 μm. The reason is that by enlarging the grinding depth, the distance of the abrasive particle tip to the final grinding surface is also enlarged. The results are consistent with a conclusion by the theoretical analysis shown in Fig. 7.

Figure 13 intuitively demonstrates the simulation results of SSD depth for different v_s/v_w. The crack depth gradually decreases with elevating the v_s/v_w ratio from Fig. 13a–d. When the ratio respectively are v_s/v_w = 500, 800, 1100, and 1400, the measured maximum crack depths in simulation at $h_i = h_m$ are 5.47, 3.84, 1.92, and 1.65 μm. According to Eq. (19), the corresponding SSD depths which can be obtained are 3.75, 2.28, 0.45, and 0.28 μm. The curve is shown in Fig. 14b, which clearly shows that the larger value of v_s/v_w can obtain the better quality of grinding surface during the grinding process. It means that when the workpiece speed is constant in grinding process, the quality of grinding surface in high wheel speed will be better than the low speed. Through the FEM simulation, it can be seen that the results are consistent with a conclusion by the theoretical analysis shown in Fig. 9.

The influences of wheel diameters on SSD and grinding surface integrity are seldom studied in existing papers, which can be approximately simulated by changing the contact trajectory length L_s. The contact trajectory length L_s increases with the increment of wheel diameter according to Eq. (4). Figure 15 intuitively describes the influences of different wheel diameters on SSD in the grinding process of BK7 glass. The wheel diameters are respectively 0.4, 0.3, 0.2, and 0.1 m from Fig. 15a–d, which is reduced, and the corresponding contact trajectory length L_s is also reduced in simulation

Table 2 Grinding parameters in simulation

Parameters	Values
Grinding depth (μm)	1, 2, 5, and 10
Wheel speed (m/s)	50, 80, 110, and 140
Workpiece speed (m/s)	0.1
Wheel diameter (m)	0.1, 0.2, 0.3, 0.4
Half apex of abrasive particle (deg)	30, 40, 50, 60

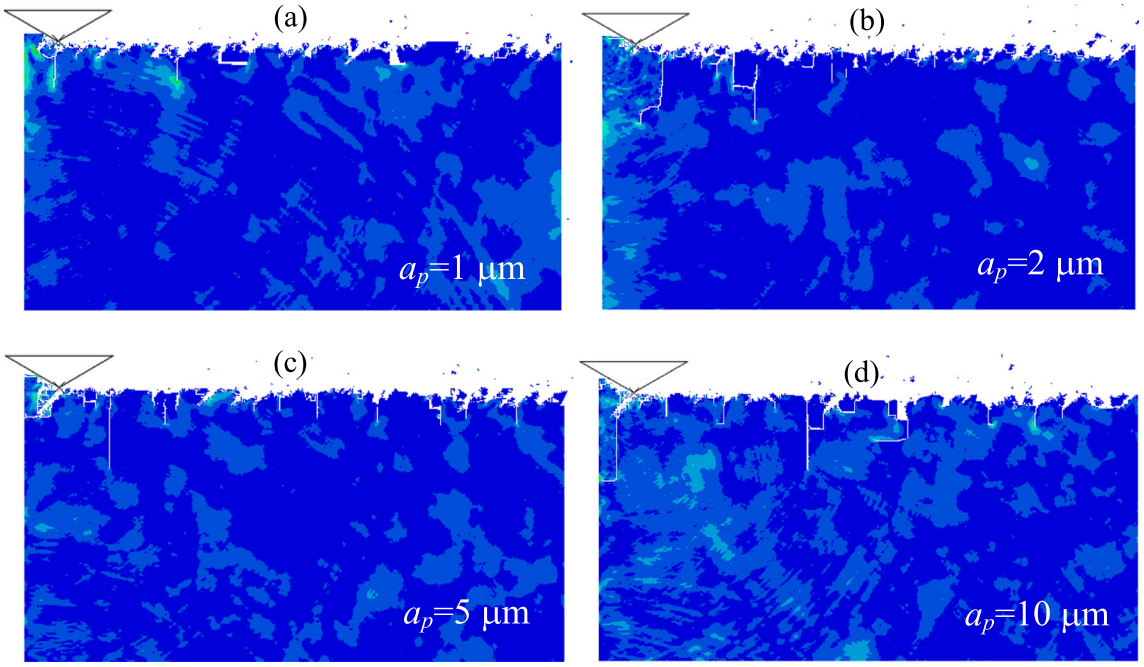

Fig. 12 Effects of different a_p on grinding process of BK7 glass for d_w = 0.2 m, v_s/v_w = 500 and α = 60°

process for a given grinding depth a_p. While grinding depth remains at a_p = 1 μm, the penetration depth h_i is kept as a constant, reducing L_s, the quality of grinding surface becomes more serious gradually which demonstrates that SSD is sensitive to the wheel diameter. The conclusions are consistent with the trends by theoretical analysis mentioned above in Fig. 8.

In addition, according to the theoretical analysis above, the different apex angles of abrasive particle can be described as the different abrasive particle sizes to investigate its effect on normal grinding force. Therefore, the effect of the half apex angles of abrasive particle α on SSD is also necessary to be investigated to better understand the effect of abrasive particle size on SSD by FEM simulation with the shape of a circular cone. Figure 16 describes the grinding process of BK7 glass with the half apex angles of abrasive particle α respectively being 30°, 40°, 50°, and 60°. The simulation results from Fig. 16a–d intuitively indicate that SSD becomes more serious

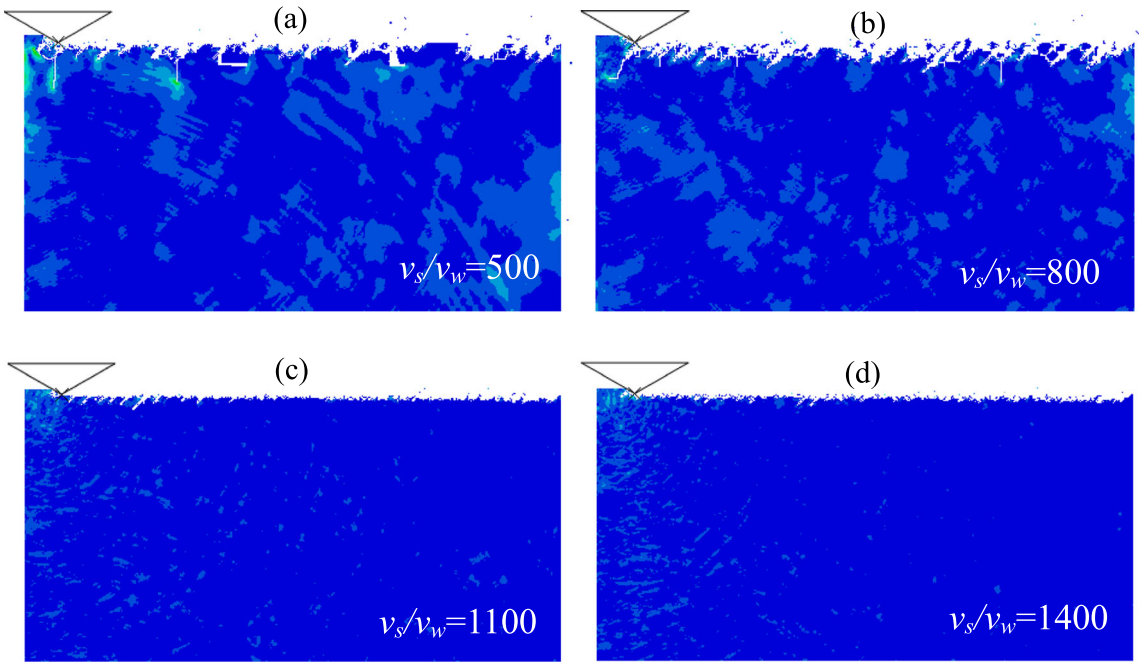

Fig. 13 Effects of different v_s/v_w on grinding process of BK7 glass for a_p = 1 μm, d_w = 0.2 m, and α = 60°

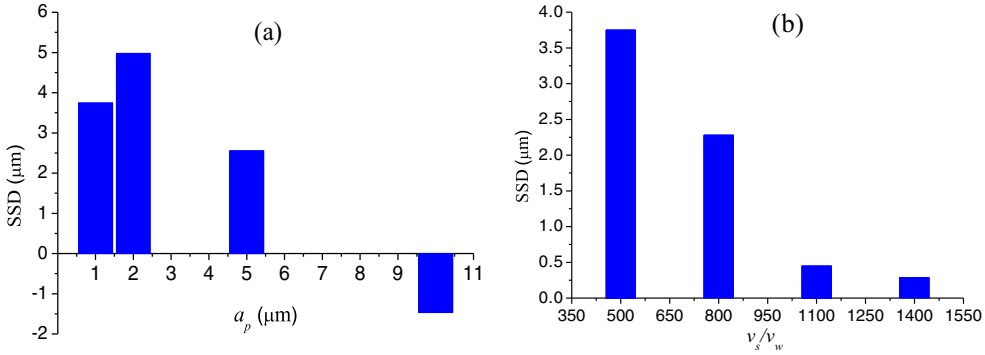

Fig. 14 SSD depth in grinding process of BK7 glass at $h_i = h_m$ for different a_p in (**a**) and v_s/v_w in (**b**)

with the increasing of the half apex angles of abrasive particle α, which means that the abrasive particle size strongly affects the surface integrity in brittle material grinding. That is the fact that the larger half apex angles of abrasive particle α leads to the larger grinding force in grinding process as shown in Fig. 5, whereas the grinding force is the main reason that leads to crack propagation when grinding brittle material in brittle fracture mode according to the works of Subramanian et al. [52]. Moreover, many relevant literatures have investigated the effect of abrasive particle size on subsurface damage. Lambropoulos [53] has estimated the effect of abrasive particle size on SSD by experimental measure, which indicated that SSD depth increases with the increment of abrasive particle size. Yao et al. [30] and Zhao et al. [54] have investigated the relationship between SSD and abrasive particle size by experimental tests, which also revealed that SSD increases with the increment of abrasive particle size. The simulation results in this study are in good agreement with those existing literatures in a certain extent. In addition, Axinte et al. [55] have experimentally investigated three different shapes of single abrasive particle (circular/square/triangular base frustum) in the grinding process of brittle materials, which indicated that the circular base frustum particle has a greater specific cutting force and produces extensive plastic deformation than those particles with square shape and triangular shape in brittle material grinding.

The FEM simulation is usually utilized to substitute the experimental method to study the practical engineering problems for the purpose of cost savings. In this paper, through combining with the theoretical analysis and the FEM simulation, the correctness of the brittle material grinding model is verified. In the actual application, the conclusion of the model can be used to guide the grinding process to achieve the optimal quality of the grinding surface.

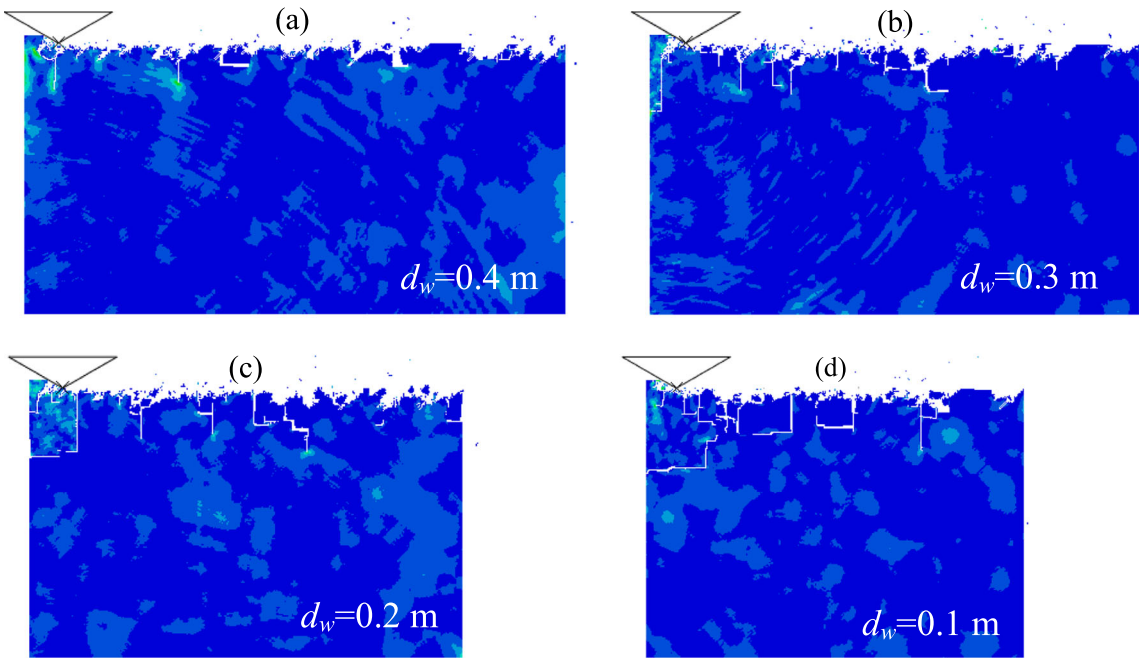

Fig. 15 Effects of different d_w on grinding process of BK7 glass for a_p = 1 μm, v_s/v_w = 500 and α = 60°

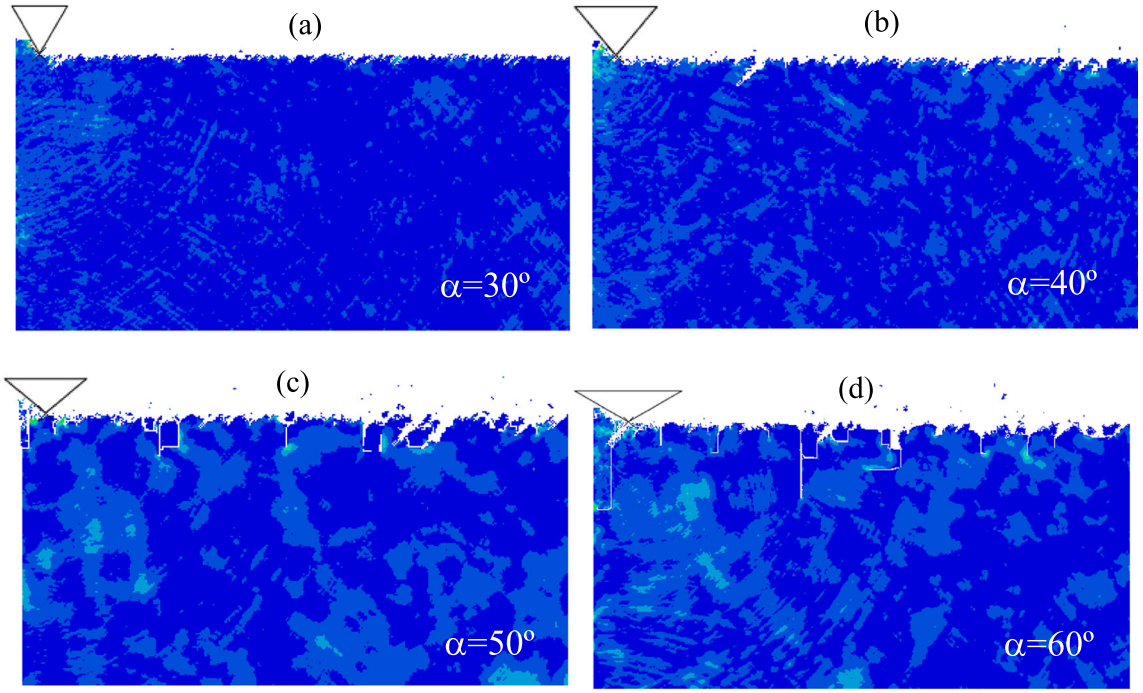

Fig. 16 Effects of different α on grinding process of BK7 glass for a_p = 10 μm, d_w = 0.2 m, and v_s/v_w = 500

4 Conclusions

In this paper, a model has been established to evaluate SSD induced by median or lateral cracks in brittle material grinding. Based on reasonable assumptions and simplifications to the material removal process, the relationship between the lateral crack and the normal grinding force can be established and the normal grinding force can be predicted in the grinding process. In addition, the effects of median and lateral cracks on SSD under different grinding parameters considering the abrasive particle rotation are studied in the grinding process of BK7 glass. Major conclusions can be obtained as follows:

1. Based on the brittle fracture mode in the grinding process, the lateral crack is the primary mechanism of material removal and chip formation, which is closely related with the normal grinding force that strongly affects SSD. In this paper, the normal grinding force is predicted according to the material removal process and the relationship between the lateral crack and the normal grinding force. In addition, the effects of grinding parameters on the normal grinding force are analyzed in detail, which indicates that the normal grinding force increases with the increment of grinding depth and the apex angle of abrasive particle decreases with the increment of wheel diameter and the v_s/v_w ratio in the grinding process of BK7 glass.
2. For the given grinding parameters, the critical brittle fracture angle θ_c is an instantaneous abrasive-workpiece contact angle at which cracks begin to appear in brittle material grinding. Moreover, the larger critical brittle fracture angle θ_c can prolong the ductile removal domain. The larger grinding depth and the smaller wheel diameter as well as the larger v_s/v_w ratio can lead to a larger critical brittle fracture angle θ_c, which is beneficial to achieve the aim of ductile processing.
3. The inclination of the median and lateral cracks along with the abrasive particle rotation in the grinding process is considered. The effects of abrasive particle rotation and grinding parameters on SSD depth have been studied in detail. The larger wheel diameter and the larger v_s/v_w ratio can cause smaller SSD depth induced by median cracks, whereas the effect of grinding depth is unapparent due to the effect of abrasive particle rotation. The smaller grinding depth and the larger wheel diameter as well as the larger v_s/v_w ratio can also obtain the smaller SSD depth induced by lateral cracks. These results can be applied to control SSD in the actual grinding process of brittle materials.
4. In FEM simulation analysis, a single abrasive particle scratching the workpiece surface is used to replace the grinding process of BK7 glass. The FEM simulation results are consistent with the theoretical analysis by comparing SSD depth for different grinding parameters to some extent, which illustrates that the theoretical analysis and the FEM simulation process are reliable.

Acknowledgments The authors would like to appreciate the support from the NNSFC (11572118 and 11372103), the Hunan Provincial Science Fund for Distinguished Young Scholars (2015JJ1006), and the Fok Ying-Tong Education Foundation, China (141005).

References

1. De Chiffre L, Kunzmann H, Peggs GN, Lucca DA (2003) Surfaces in precision engineering, microengineering and nanotechnology. CIRP Ann-Manuf Technol 52(2):561–577
2. Arif M, Rahman M, San WY (2011) Analytical model to determine the critical feed per edge for ductile–brittle transition in milling process of brittle materials. Int J Mach Tools Manuf 51(3):170–181
3. Camp DW, Kozlowski MR, Sheehan LM, Nichols MA, Dovik M, Raether RG, Thomas IM (1998) Subsurface damage and polishing compound affect the 355-nm laser damage threshold of fused silica surfaces. International Society for Optics and Photonics :356–364
4. Giovanola JH, Finnie I (1980) On the machining of glass. J Mater Sci 15(10):2508–2514
5. Bifano TG, Dow TA, Scattergood RO (1991) Ductile-regime grinding: a new technology for machining brittle materials. J Manuf Sci E-T ASME 113(2):184–189
6. Cai MB, Li XP, Rahman M (2007) Study of the mechanism of nanoscale ductile mode cutting of silicon using molecular dynamics simulation. Int J Mach Tools Manuf 47(1):75–80
7. Liu K, Li XP, Liang SY (2007) The mechanism of ductile chip formation in cutting of brittle materials. Int J Adv Manuf Technol 33(9–10):875–884
8. Cao JG, Wu YB, Li JY, Zhang QJ (2016) Study on the material removal process in ultrasonic-assisted grinding of SiC ceramics using smooth particle hydrodynamic (SPH) method. Int J Adv Manuf Technol 83(5–8):985–994
9. Arif M, Xinquan Z, Rahman M, Kumar S (2013) A predictive model of the critical undeformed chip thickness for ductile–brittle transition in nano-machining of brittle materials. Int J Mach Tools Manuf 64:114–122
10. Li BZ, Ni JM, Yang JG, Liang SY (2014) Study on high-speed grinding mechanisms for quality and process efficiency. Int J Adv Manuf Technol 70(5–8):813–819
11. Bach H, Neuroth N (1998) The properties of optical glass. Springer Science & Business Media
12. Lawn BR, Fuller ER (1975) Equilibrium penny-like cracks in indentation fracture. J Mater Sci 10(12):2016–2024
13. Lawn BR, Swain MV (1975) Microfracture beneath point indentations in brittle solids. J Mater Sci 10(1):113–122
14. Wang CC, Fang QH, Chen JB, Liu YW, Jin T (2015) Subsurface damage in high-speed grinding of brittle materials considering kinematic characteristics of the grinding process. Int J Adv Manuf Technol 83(5–8):937–948
15. Chen JB, Fang QH, Li P (2015) Effect of grinding wheel spindle vibration on surface roughness and subsurface damage in brittle material grinding. Int J Mach Tools Manuf 91:12–23
16. Lawn BR, Evans AG, Marshall DB (1980) Elastic/plastic indentation damage in ceramics: the median/radial crack system. J Am Ceram Soc 63(9–10):574–581
17. Marshall DB, Lawn BR, Evans AG (1982) Elastic/plastic indentation damage in ceramics: the lateral crack system. J Am Ceram Soc 65(11):561–566
18. Turchetta S (2009) Cutting force on a diamond grit in stone machining. Int J Adv Manuf Technol 44(9–10):854–861
19. Agarwal S, Rao PV (2008) Experimental investigation of surface/subsurface damage formation and material removal mechanisms in SiC grinding. Int J Mach Tools Manuf 48(6):698–710
20. Agarwal S, Rao PV (2010) Grinding characteristics, material removal and damage formation mechanisms in high removal rate grinding of silicon carbide. Int J Mach Tools Manuf 50(12):1077–1087
21. Feng J, Chen P, Ni J (2013) Prediction of grinding force in microgrinding of ceramic materials by cohesive zone-based finite element method. Int J Adv Manuf Technol 68(5–8):1039–1053
22. Gu WB, Yao ZQ, Liang XG (2011) Material removal of optical glass BK7 during single and double scratch tests. Wear 270(3): 241–246
23. Gu WB, Yao ZQ (2011) Evaluation of surface cracking in micron and sub-micron scale scratch tests for optical glass BK7. J Mech Sci Technol 25(5):1167–1174
24. Wang CC, Chen JB, Fang QH, Liu F, Liu YW (2016) Study on brittle material removal in the grinding process utilizing theoretical analysis and numerical simulation. Int J Adv Manuf Technol :1–12
25. Huang H, Yin L, Zhou LB (2003) High speed grinding of silicon nitride with resin bond diamond wheels. J Mater Process Technol 141(3):329–336
26. Chen JY, Shen JY, Huang H, Xu XP (2010) Grinding characteristics in high speed grinding of engineering ceramics with brazed diamond wheels. J Mater Process Technol 210(6):899–906
27. Liu DF, Cong WL, Pei ZJ, Tang YJ (2012) A cutting force model for rotary ultrasonic machining of brittle materials. Int J Mach Tools Manuf 52(1):77–84
28. Zhang CL, Zhang JF, Feng PF (2013) Mathematical model for cutting force in rotary ultrasonic face milling of brittle materials. Int J Adv Manuf Technol 69(1–4):161–170
29. Xiao XZ, Zheng K, Liao WH (2014) Theoretical model for cutting force in rotary ultrasonic milling of dental zirconia ceramics. Int J Adv Manuf Technol 75(9–12):1263–1277
30. Yao ZQ, Gu WB, Li KM (2012) Relationship between surface roughness and subsurface crack depth during grinding of optical glass BK7. J Mater Process Technol 212(4):969–976
31. Lawn B, Wilshaw R (1975) Indentation fracture: principles and applications. J Mater Sci 10(6):1049–1081
32. Marinescu ID, Rowe WB, Dimitrov B, Inaski I (2004) Tribology of abrasive machining processes. Elsevier
33. Malkin S (1989) Grinding technology: theory and applications of machining with abrasives (Ellis Horwood limited. Chichester, England
34. Cook RF, Pharr GM (1990) Direct observation and analysis of indentation cracking in glasses and ceramics. J Am Ceram Soc 73(4):787–817
35. Nakamura M, Sumomogi T, Endo T (2003) Evaluation of surface and subsurface cracks on nano-scale machined brittle materials by scanning force microscope and scanning laser microscope. Surf Coat Tech 169:743–747
36. Gu WB, Yao ZQ, Li K (2011) Evaluation of subsurface crack depth during scratch test for optical glass BK7. P I Mech Eng C-J Mec :0954406211412458
37. Gu WB, Yao ZQ, Li HL (2011) Investigation of grinding modes in horizontal surface grinding of optical glass BK7. J Mater Process Technol 211(10):1629–1636
38. Shaw MC (1996) Principles of abrasive processing, vol 13. Oxford University Press
39. Mayer JE, Fang GP, Kegg RL (1994) Effect of grit depth of cut on strength of ground ceramics. CIRP Ann-Manuf Techn 43(1):309–312
40. Young HT, Chen DJ (2006) Online dressing of profile grinding wheels. Int J Adv Manuf Technol 27(9–10):883–888
41. Sahu P, Sagar R (2006) Development of abrasive cut-off wheel having side grooves. Int J Adv Manuf Technol 31(1–2):37–40
42. Ma Y, Lou ZF (2005) Abrasive technology of single-crystal diamond by diamond abrasive wheel. Key Eng Mater 291:21–26
43. Jackson MJ, Davis CJ, Hitchiner MP, Mills B (2001) High-speed grinding with CBN grinding wheels—applications and future technology. J Mater Process Technol 110(1):78–88
44. Hecker RL, Liang SY (2003) Predictive modeling of surface roughness in grinding. Int J Mach Tools Manuf 43(8):755–761
45. Li K, Liao TW (1996) Surface/subsurface damage and the fracture strength of ground ceramics. J Mater Process Technol 57(3):207–220

46. Park HW, Liang SY (2008) Force modeling of micro-grinding incorporating crystallographic effects. Int J Mach Tools Manuf 48(15):1658–1667
47. Zhu DH, Yan SJ, Li BZ (2014) Single-grit modeling and simulation of crack initiation and propagation in SiC grinding using maximum undeformed chip thickness. Comp mater Sci 92:13–21
48. Inasaki I (1996) Grinding process simulation based on the wheel topography measurement. CIRP Ann-Manuf Technol 45(1):347–350
49. Chen MJ, Zhao QL, Dong S, Li D (2005) The critical conditions of brittle–ductile transition and the factors influencing the surface quality of brittle materials in ultra-precision grinding. J Mater Process Technol 168(1):75–82
50. Sun DW, Sealy MP, Liu ZY, Fu CH, Guo YB, Fang FZ, Zhang B (2015) Finite element analysis of machining damage in single-grit grinding of ceramic knee implants. Procedia Manufacturing 1:644–654
51. Hibbit D, Karlsson B, Sorenson P (2010) Abaqus/explicit user's manual, version 6.10, Abaqus Inc
52. Subramanian K, Ramanath S, Tricard M (1997) Mechanisms of material removal in the precision production grinding of ceramics. J Manuf Sci E-T ASME 119(4A):509–519
53. Lambropoulos JC (2000) From abrasive size to subsurface damage in grinding. Convergence 8:1–3
54. Zhao B, Gao S, Kang RK, Zhu XL, Guo DM (2016) Surface and subsurface integrity of glass-ceramics induced by ultra-precision grinding. Adv Mater Res 1136:497–502
55. Axinte D, Butler-Smith P, Akgun C, Kolluru K (2013) On the influence of single grit micro-geometry on grinding behavior of ductile and brittle materials. Int J Mach Tools Manuf 74:12–18